Evaluation of fouling resistances during the ultrafiltration of whey model solutions

María-José Corbatón-Báguena, Silvia Álvarez-Blanco, María-Cinta Vincent-Vela*

Department of Chemical and Nuclear Engineering, Universitat Politècnica de València, C/Camino de Vera s/n 46022 Valencia, Spain

*Corresponding author: mavinve@iqn.upv.es

Tel: 96 387 93 87 (Ext.:79387)

Abstract

In the last decades, the ultrafiltration of whey has grown in importance as a "green" technique. However, since fouling is an important drawback, researchers focused on its prediction by mathematical models. In this work, three ultrafiltration membranes of different molecular weight cut-offs and materials were used to ultrafilter whey model solutions of different protein concentrations. As a novelty, a resistance-in-series model that accounts for the time evolution of the fouling resistances was considered. The results demonstrated that the higher the protein and salt concentrations in the feed solutions were, the greater the fouling degree was. The resistance-in-series model was accurately fitted to the experimental data for each membrane and feed solution used. The results showed that the resistance due to adsorption dominated the first minutes of operation, while the membrane characteristics (surface roughness and hydrophilicity/hydrophobicity) played an important role in the growth of the cake layer.

Keywords: Ultrafiltration; whey model solutions; membrane fouling; hydraulic resistance.

1. Introduction

During the manufacture of cheese and casein in the dairy industries, great volumes of a greenish-yellow liquid by-product named "whey" are obtained (Garrido et al., 2016; Carvalho et al., 2013). According to the literature, 8 to 9 kg of whey are produced per 1-2 kg of cheese, resulting in a worldwide production of about 180-190 millions ton/year (Baldasso et al., 2011). Traditionally, whey has been considered as a dairy wastewater. It has a high biological and chemical oxygen demand (of about 27-60 and 50-102 g O_2/L, respectively), thus it cannot be drained without a treatment. On the other hand, it can be reused as food supplement for livestock, organic fertiliser or as a biogas source (Carvalho et al., 2013; Chandrapala et al., 2016). Moreover, in the last decades, as a result of their outstanding properties, the recovery and fractionation of whey components is being performed (Acevedo-Correa, 2010). Among the different whey components, proteins can be remarked. Their biological, nutritional and functional properties make them attractive for being used in other industries, such as the food, pharmaceutical or cosmetics ones. These properties include their emulsification, gelling and foaming ability and their antioxidant and antimicrobial character (Ramchandran and Vasiljevic, 2013).

In the last years, membrane separation processes have grown in interest in the dairy industry, since they are considered as "green" technologies. Within these processes, ultrafiltration can be highlighted, as it shows a wide range of applications, such as the purification or fractionation of proteins (Wen-quiong et al., 2017; Zin et al., 2016), the production of whey protein concentrates and isolates with protein contents greater than 35 and 85 %, respectively (Kazemimoghadam and Mohammadi, 2006) and the production of

a lactose-enriched stream (permeate) (Metsämuuronen and Nyström, 2009). Among the numerous advantages of membrane separation processes, the following can be remarked (Zin et al., 2016; Daufin et al., 2001): they are modular processes, easy to scale up and adapt to different industrial requirements, no addition of chemicals is needed to perform the separation and the desired products are obtained with high quality since membrane processes are performed at mild operating conditions.

Nevertheless, the main drawback of ultrafiltration processes is membrane fouling, which gradually reduces the permeate flux and increases the hydraulic resistance and thus the overall process productivity diminishes (Cheryan and Álvarez, 1995). Regarding the dairy industry, proteins are the main compounds responsible for membrane fouling (Argüello et al, 2003). This phenomenon is due to the foulant-foulant and foulant-membrane interaction forces and depends on different factors such as the pH, the temperature and the composition of the feed solution, the characteristics of the membrane (pore size and material) and the operating conditions (transmembrane pressure and crossflow velocity) (Wang et al., 2012). Due to the great influence that the decline of permeate flux has on process productivity, research has been focused on the prediction of the time evolution of permeate flux by means of the development of mathematical models (Ho and Zydney, 2000; Choi et al., 2000; Bolton et al., 2006; Chen and Kim, 2006; Mondal and De, 2010). Among the different mathematical models available in the literature, semi-empirical models are the most appropriate to both achieve accurate predictions and determine the predominant membrane fouling mechanisms (Salahi et al., 2010; Vincent-Vela et al., 2009; Mah et al., 2012). These models are based on simplified equations of scientific laws that consider several fitting parameters with physical meaning. The resistance-in-series model is the most often used. For instance, Choi et al. (2000) characterized the permeate flux

decline during the microfiltration of BSA adsorbed microspheres by means of a resistance-in-series model that considered two fouling resistances: the resistance due to the formation of a cake layer on the membrane surface and that due to the deposition of foulant molecules inside the membrane porous structure. Carrère et al. (2002) fitted a resistance-in-series model to the experimental data obtained during the microfiltration of lactic acid fermentation broths. As fouling resistances, they considered the concentration polarization resistance, the adsorption resistance and the cake formation one. As main results, they demonstrated that resistances due to concentration polarization and adsorption were the predominant ones. Carbonell-Alcaina et al. (2016) used a resistance-in-series model to determine the fouling mechanisms responsible for flux decline during the ultrafiltration of table olive storage wastewaters. These authors included as fouling resistances the one due to the adsorption of foulants on the membrane surface and that related to cake formation. They reported that pore blocking, adsorption and cake formation were the fouling resistances responsible for permeate flux decline.

As the fouling resistances due to adsorption and concentration polarization and cake formation phenomena are the predominant ones in the ultrafiltration of protein based solutions (Katsoufidou et al., 2005), the main objective of this work was to relate the model parameters of a resistance-in-series model to the different membranes and feed solutions tested. The solutions were composed of BSA and BSA + $CaCl_2$, respectively and a real whey protein concentrate (WPC) was considered as well. Three different membranes (in terms of molecular weight cut-off, MWCO, and material) were used, so that, as a novel aspect, the values of the fitting parameters could be related not only to the characteristics of the feed solutions, but also to these of the membranes (MWCO and hydrophilicity/hydrophobicity). As a novelty, the temporal evolution of the

abovementioned model parameters was determined and the predominance of each fouling resistance as a function of time, feed solution and membrane tested was investigated.

2. Modelling

2.1. Resistance-in-series model

The resistance-in-series model considered in this work takes into account the contribution of four different hydraulic resistances on permeate flux evolution with time: the original membrane resistance, the resistance due to the adsorption of solute on the membrane surface and also on the pore walls, the resistance due to the concentration polarization and finally, the resistance due to the growth of the cake layer formed by the deposited solute molecules (Carrère et al., 2002; Carbonell-Alcaina et al., 2016). Thus the general equation for the resistance-in-series model is Eq. 1:

$$J_p = \frac{\Delta P}{\mu \cdot \left(R_m + R_{ads} + R_{cp} + R_{cl}\right)} \qquad \text{Eq. 1}$$

where J_p is the permeate flux at each time, ΔP is the transmembrane pressure, μ is the viscosity of the feed solution, R_m is the resistance of the original membrane, R_{ads} is the resistance due to adsorption on membrane surface and on the pore walls, R_{cp} is the resistance due to concentration polarization and R_{cl} is the resistance due to the growth of the cake layer.

According to previous studies (Carrère et al., 2002; Carrère et al., 2001; Juang et al., 2008), the resistances due to adsorption and concentration polarization have an exponential time

dependence that makes these resistances grow at a rate constant b up to a steady-state value $R_{ads,\ ss} + R_{cp,\ ss}$. Therefore the general mathematical equation for these resistances is expressed as in Eq. 2:

$$R_{ads} + R_{cp} = \left(R_{ads,ss} + R_{cp,ss}\right) \cdot \left(1 - exp\left(-b \cdot t\right)\right) \qquad \text{Eq. 2}$$

Where $R_{ads,ss}$ is the resistance due to solute adsorption at the steady-state, $R_{cp,ss}$ is the resistance due to concentration polarization at the steady-state, b is the rate constant at which the resistances grow and t is the filtration time.

On the other hand, the same studies defined the resistance caused by the formation of a cake layer on the membrane surface by means of a pressure-dependent relationship as in Eq. 3:

$$R_{cl} = \left(\frac{m_{dep}}{A_m}\right) \cdot \alpha \qquad \text{Eq. 3}$$

Where R_{cl} is the resistance due to cake formation, m_{dep} is the protein mass deposited on the membrane surface, A_m is the membrane area and α is the specific cake resistance.

The protein mass deposited on the membrane surface can be determined by means of a mass balance equation and considering that (i) the protein concentration at the membrane wall is greater than the protein concentration in the retentate stream and (ii) the temporal variation of the deposited mass is zero when the end of the tests is achieved, as follows (Juang et al., 2008):

$$\frac{dm_{dep}}{dt} = A_m \cdot C_r \cdot \left(J_p - J_{p,f}\right) \qquad \text{Eq. 4}$$

Where C_r is the protein concentration in the retentate stream and $J_{p,f}$ is the permeate flux at the end of the tests.

By substituting Eqs. 2-4 in Eq. 1, the general equation for the resistance-in-series model is Eq. 5:

$$J_p = \frac{\Delta P}{\mu \cdot \left(R_m + \left(R_{ads,ss} + R_{cp,ss}\right) \cdot \left(1 - exp\left(-b \cdot t\right)\right) + \left(\frac{m_{dep}}{A_m}\right) \cdot \alpha \right)} \qquad \text{Eq. 5}$$

3. Experimental

3.1. Experimental set-up

Experiments were carried out in a laboratory scale ultrafiltration plant (VF-S11 model, Orelis, France). This plant was equipped with a temperature control system, a 10 L stainless steel feed tank, a volumetric pump with speed regulation to select the crossflow velocity, a manometer at each side of the membrane module to maintain the transmembrane pressure constant and a scale (with an accuracy of ±0.001 g). A complete scheme of the experimental set-up can be found in Corbatón-Báguena et al. (2014).

3.2. Membranes and chemicals

Three different ultrafiltration membranes were used to perform the experiments: a monotubular ZrO_2-TiO_2 membrane of 15 kDa (Inside-Céram, TAMI Industries, France) and two flat-sheet membranes of 5 and 30 kDa (Microdyn Nadir, Germany) with active surface of polyethersulfone and permanently hydrophilic polyethersulfone, respectively. The effective area of such membranes was 35.5 cm^2 in the case of the 15 kDa membrane and 100 cm^2 for the polymeric membranes. The dimensions of the 15 kDa membrane were the following: 20 cm in length, 0.6 cm of internal diameter and 1 cm of external diameter.

The abovementioned membranes were used to ultrafilter three different types of whey model solutions, which contained BSA (A3733, Sigma-Aldrich, Germany), a mixture of BSA and $CaCl_2$ (Panreac, Spain) and a commercial WPC with a total protein content of 45 w% (Industrias Lácteas Asturianas, Spain). The composition of the commercial WPC is shown in Table 1. The chemicals and the commercial WPC were all supplied in powder form and thus they were dissolved in deionized water to obtain the following concentrations: 10 g/L of BSA, 1.65 g/L of $CaCl_2$ and 22.2 (10 g/L of total proteins), 33.3 (15 g/L of total proteins) and 44.4 g/L (20 g/L of total proteins) of WPC, respectively. These whey model solutions were prepared with no pH adjustment and had pH values in the range of 5.97-6.5. No significant variations in pH were observed during the filtration experiments.

The minimum protein concentration selected of 10 g/L was chosen according to the protein composition of typical sweet cheese whey, which was about 1 w/w% of the total solid content (Goulas and Grandison, 2008).

Regarding membrane and solute charges, it was reported by the authors that the isoelectric points of BSA and WPC solutions were, 4.9 and 4.6, respectively. This means that, with no pH adjustment, all molecules in the feed solutions tested were negatively charged at the pH used in this study (about 7). In addition, several authors reported that the isoelectric points of the polymeric and ceramic membranes were about, 3 and 6.2, respectively (Fernández et al., 2010; Labbez et al., 2002). These values indicated that all the three membranes used and the solutes were negatively charged at the pH of the feed solutions and thus, there is an electrostatic repulsion between them.

3.3. Experimental procedure

Firstly, unused original membranes were characterized in terms of water permeability and membrane resistance (R_m) using deionized water. According to Eq. 1, when deionized water is used as feed, R_{ads}, R_{cp} and R_{cl} are equal to zero, and the resistance of the original membranes can be calculated from the measurements of permeate flux. The value of R_m was considered as constant for each membrane and all the feed solutions tested. Then, the membranes were used to ultrafilter the different feed solutions. The ultrafiltration plant was operated in total recycle mode at the following experimental conditions: 2 bar, 2 m/s and 25 ºC. During the total time the experiments were running, permeate flux was monitored and thus the temporal variation of the total hydraulic resistance could be determined. The selected experimental conditions corresponded to those typically used when ultrafiltering whey (Matzinos and Álvarez, 2002).

Once the experimental data was recorded, the degree of fouling was calculated by comparing the values of permeate flux at the beginning of the experiments and at the end of the tests (García-Ivars et al., 2016). Eq. 7 shows the calculation of the degree of fouling:

$$FD\ (\%) = \frac{J_{p,0} - J_{p,f}}{J_{p,0}} \cdot 100 \qquad \text{Eq. 7}$$

Where FD is the degree of fouling expressed as percentage and $J_{p,0}$ is the initial permeate flux.

3.4. Statistical and fitting procedure

In order to establish if statistically significant differences were obtained among the degree of fouling for the different feed solutions and membranes tested, the Least Significant Difference (LSD) test was carried out by means of the Statgraphics Centurion XVI software. This statistical analysis compares two means and calculates the smallest significant difference, representing it in an interval around each mean. When the difference between such means is larger than the LSD interval, this indicates that the means statistically differ one from each other (Williams and Abdi, 2010). Graphically, this significance can be observed in the overlapping of the LSD intervals of both means: if the two intervals do not overlap each other, there is a statistically significant difference between the means studied. For this analysis, each ultrafiltration experiment performed with each membrane and whey model solution was repeated ten times and the confidence interval used was 95 % in all cases.

In addition, the mathematical model explained in Section 2 was fitted to the experimental data using the Genfit algorithm from MathCad® software. This mathematical function is based on a version of the Levenberg-Marquadt curve-fitting method, which consists on a least-squares minimization, i.e. the difference between the experimental and predicted data is minimized. The fitting accuracy was evaluated by means of the regression coefficient (R^2) and the standard deviation (SD).

4. Results and discussion

4.1. Ultrafiltration of whey model solutions

The values of R_m for the 5, 15 and 30 kDa membranes were $9.453 \cdot 10^{12}$, $5.001 \cdot 10^{12}$ and $3.794 \cdot 10^{12}$ m^{-1}, respectively.

The temporal increase of the total hydraulic resistance for all the feed solutions considered and each membrane tested is shown in Fig. 1. For all the membranes it was observed that, for those solutions that had the same protein concentration (10 g/L), the largest values of the resistance at the end of the filtration process were obtained when the solutions contained salts (BSA + $CaCl_2$ and WPC 22.2 g/L solutions). Moreover, the greatest increase in the resistance values during the elapse of the ultrafiltration tests was also observed for these solutions. Therefore the presence of salts in the feed solution led to a more severe membrane fouling. The reason for that is the effect that inorganic salts, especially calcium, have on proteins structure. For instance, Mo et al. (2008) studied the influence of several cations on membrane fouling due to BSA. They reported that flux decline was much higher when calcium was added to the BSA feed solution (36 % at pH 7)

in comparison with the flux decline achieved when sodium was used (12 % at pH 7). This was explained taking into account that calcium enhances the crosslinking between adjacent carboxyl groups of different protein chains, which results in a denser fouling layer. In the same way, Mession et al. (2013) demonstrated that the presence of calcium in a protein system allows the formation of salt bridges between protein chains. Thus protein molecules join together and form large agglomerates. In addition, the higher concentration of salts in the WPC 22.2 g/L solution compared to the BSA + $CaCl_2$ one favours the more severe membrane fouling. Thus the value of the total hydraulic resistance was greater when the WPC 22.2 g/L solution was ultrafiltered. Related to this, Fig. 2 shows the values of the fouling degree at the end of the filtration process and the resulting LSD intervals for the different membranes and feed solutions tested. For each membrane considered and the whey model solutions with a protein concentration of 10 g/L (BSA, BSA + $CaCl_2$ and WPC 22.2 g/L solutions), the lowest fouling degree was observed for the BSA solutions.

On the other hand, comparing the results obtained when protein concentration increased in the feed solution (WPC 22.2, 33.3 and 44.4 g/L solutions), Fig. 1 shows that higher values of total hydraulic resistance were achieved as protein concentration increased. This fact demonstrated that the greater amount of proteins in the feed solution resulted in a tighter and denser cake layer on the membrane surface and thus resulted in a more severe membrane fouling (Zhang et al., 2016; Yu et al., 2014). The same trend can be observed from Fig. 2a and b for the 5 and 15 kDa membranes. However, Fig. 2c shows that, in the case of the 30 kDa membrane, no statistically significant difference was found among the three LSD intervals obtained for the different WPC solutions. This means that an increase in protein concentration did not result in a significant increase in membrane fouling in this case and it may be due to the hydrophilic nature of this membrane, according to the

membrane manufacturer. Hydrophobic molecules such as the hydrophobic aminoacid residues of proteins tend to preferentially deposit on hydrophobic surfaces (like the surface of hydrophobic membranes) rather than remaining exposed to the aqueous solution (Ghosh, 2003). Comparing the three membranes used in this work, the less hydrophobic one was the 30 kDa membrane and thus it might repel the protein molecules from being deposited on the membrane surface to a certain extent. This fact has been confirmed by other authors in their works on membrane material modification and membrane fabrication. For instance, García-Ivars et al. (2014) performed ultrafiltration experiments with polyethersulfone membranes of about 30 kDa and using polyethylene glycol as feed solution. After 2 hours, the modified hydrophilic polyethersulfone membrane showed the highest permeate flux and the lowest flux reduction due to fouling (about 14 %) in comparison with the unmodified hydrophobic polyethersulfone (achieving a fouling degree of about 30 %). This demonstrated the better antifouling properties that the more hydrophilic membrane had. In addition, Rahimpour and Madaeni (2010) tested different polyethersulfone membranes with non-skim milk to investigate their fouling behaviour. They reported that the permeate flux decline obtained with a hydrophilic polyethersulfone membrane was 16 %, while this parameter increased up to a value of 40 % in the case of the more hydrophobic membrane. The hydrophilic nature of the 30 kDa membrane was also responsible for the low permeate flux decline at the end of the ultrafiltration test for all the feed solutions considered (Figs. 1 and 2c).

On the other hand, rougher surfaces favour the accumulation of foulant molecules on them and suffer a more severe fouling (Bird et al., 2008). In this case, despite the hydrophilic nature of the ceramic membrane used in this study (due to the composition of its active layer), the 15 kDa membrane has much greater membrane surface roughness (17.900 nm)

than the other two membranes (1.657 nm for the 30 kDa membrane and 0.487 nm for the 5 kDa one), as reported in a previous work (Corbatón-Báguena et al., 2015). Therefore when the concentration of proteins in the feed solution increased, the concentration of proteins accumulated and deposited on the membrane surface increased and the fouling degree achieved at the end of the ultrafiltration process increased as well. This fact is clearly observed comparing Fig. 2b (for the 15 kDa ceramic membrane) with Figs. 2a and c (for the polymeric ones). The fouling degree of the 15 kDa membrane was the greatest for all the whey model solutions tested. In addition, for this membrane the difference between the fouling degree obtained with BSA solutions and that obtained with the WPC 44.4 g/L solutions was the highest (49.61 %) compared to the other membranes (26.03 % for the 30 kDa membrane and 31.09 % for the 5 kDa membrane).

4.2. Resistance-in-series model

Using the general equation for the resistance-in-series model (Eq. 5), the predicted evolution of the total hydraulic resistance with time was determined and it is depicted in Fig. 1. In this figure, the results predicted by the model are compared with the experimental data. The values of the model parameters for each experimental condition are included in Table 2. Regarding the values of the fouling resistances R_{ads}+ R_{cp} and R_{cl} at the end of the tests, it can be observed that both resistances increased when increasing the amount of protein and salts in the feed solutions (from BSA to WPC 44.4 g/L). This is related to the more severe fouling that an increase in the concentration of these molecules caused on the membranes. For instance, Rajabzadeh et al. (2010) investigated the effect of protein concentration on the fouling of a polysulfone 100 kDa ultrafiltration membrane when soy protein extracts were used as feed. These authors showed that an increase in

protein concentration in the feed solution by a factor of 4 resulted in an increase in the fouling resistances by a factor of 2. Carrère et al. (2001) microfiltered lactic acid fermentation broths with a 0.1 μm ceramic membrane and demonstrated that the fouling resistance due to adsorption and concentration polarization increased when fouling conditions became more severe (increasing the transmembrane pressure applied).

On the other hand, comparing the values of the fouling resistances for the same feed solution and the different membranes tested, it can be observed that the values obtained for the 30 kDa membrane were the lowest. This is due to the greater hydrophilic nature of this membrane in comparison with the other two used in the experiments, as it was previously commented.

In Table 2 it can be observed that the values of parameter b (the rate of growth of the resistances due to adsorption and concentration polarization) are very similar for the different membranes and feed solutions. This result is in agreement with previous studies where an exponential equation was used to express the temporal evolution of the resistance due to adsorption and concentration polarization. Different authors obtained an almost constant value of the parameter b independently of the operating conditions considered (Carrère et al., 2001). Regarding the values of the specific cake resistance obtained for the different membranes and whey model solutions tested, previous works reported that this parameter increased as the size of the molecules in the feed solution decreased (Lee and Clark, 1998; Salinas-Rodríguez et al., 2015). This pattern can be clearly distinguished when comparing the values of α for BSA and WPC 22.2 g/L solutions and the same membrane. For all the membranes considered, α increased when smaller molecules were introduced in the feed solution (for instance, α-lactalbumin and β-lactoglobulin, which are

present in the WPC solutions and are smaller than BSA). In addition, other authors investigated the influence that the ionic strength of the feed solution has on the values of the specific cake resistance (Boerlage et al., 2003; Bacchin et al., 1996). According to their works, an increase in the ionic strength of the environment leads to a reduction in the distance between hydrophobic molecules in the formed cake and a compression in the double layer around these molecules and the membrane surface, thus increasing the specific cake resistance (Boerlage et al., 2003). However, once the ionic strength achieved a maximum value, a further increase in the ionic strength can favour the aggregation of molecules into larger size particles, forming a less compacted cake and thus reducing the specific cake resistance (Bacchin et al., 1996). This pattern is in a good agreement with the parabolic trend observed for the 5 and 30 kDa membranes when comparing the values of α for the different WPC solutions tested.

The fitting accuracy of the resistance-in-series model in terms of R^2 and SD is shown in Table 3. For all the membranes and feed solutions tested, the model accurately fitted the experimental data, with values of R^2 ranging from 0.956 to 0.996 and values of SD of 0.005 to 0.027. The temporal evolution of the predicted fouling resistances observed for the 5, 15 and 30 kDa membranes when using WPC solutions at the highest concentration tested (44.4 g/L) is shown in Figs. 3 and 4. It is worthy to note that, as explained before, the rougher surface of the 15 kDa membrane resulted in a greater accumulation of proteins on it and thus the predominant fouling resistance at the end of the experiment with WPC 44.4 g/L was the one due to cake layer formation. Contrarily, the hydrophilic nature of the 30 kDa membrane prevents its surface from proteins accumulation and therefore the value of the cake resistance was the lowest in comparison with that corresponding to the 5 and 15 kDa membranes. As other authors previously described, the fouling phenomenon due to

the adsorption of foulant molecules on the membrane surface occurred at low time scales and therefore they are the main responsible for the sharply decrease in permeate flux and the rapid initial increase in the total hydraulic resistance (Choi et al., 2000). However, as the ultrafiltration time advances, the initial pattern for both permeate flux and hydraulic resistance slows down due to the gradually growth of the cake layer. This pattern can be distinguished in Figs. 3 and 4 for the three membranes used, where it can be observed that the maximum value of the resistance due to adsorption and concentration polarization was achieved at very low time scales, while the growth of the cake resistance was much slower.

5. Conclusions

- The resistance-in-series model accounting for the time evolution of two fouling resistances (the resistance due to adsorption and concentration polarization and the resistance due to cake layer formation) fitted with high accuracy the experimental data obtained for all the membranes tested and the different whey model solutions used at a transmembrane pressure of 2 bar and a crossflow velocity of 2 m/s.

- The higher the protein concentration in the feed solution was, the greater the fouling degree was for all the membranes tested. In the same way, the presence of inorganic salts, especially calcium, in the feed solution led to a more severe membrane fouling, due to their binding effect on proteins.

- The values of the fouling resistances increased with protein concentration and with the presence of salts. In addition, the resistance due to adsorption and concentration polarization was predominant during the first minutes of operation for all the

membranes and feed solutions tested, as it sharply increased with time. However, the resistance due to the cake formation increased over the entire ultrafiltration time, being predominant at the end of the filtration process for the 15 kDa membrane. In the case of the 30 kDa membrane, the resistance due to adsorption and concentration polarization was the main responsible for membrane fouling for all the feed solutions tested.

- The 30 kDa membrane showed the lowest fouling degree and fouling resistances values due to the combination of low membrane surface roughness and hydrophilic nature, which resulted in better antifouling properties compared to the other membranes used.

Acknowledgements

The authors of this work wish to gratefully acknowledge the financial support provided by the Spanish Ministry of Science and Innovation through its project CTM2010-20186.

Nomenclature

List of symbols

A_m	Membrane area (m^2)
b	Rate of growth of the resistances due to adsorption and concentration polarization (s^{-1})
C_r	Protein concentration in the retentate stream (g/L)

J_p	Permeate flux at a certain time ($L/m^2 \cdot h$)
$J_{p,0}$	Permeate flux at the initial time ($L/m^2 \cdot h$)
$J_{p,f}$	Permeate flux at the end of the test ($L/m^2 \cdot h$)
m_{dep}	Protein mass deposited on the membrane surface (kg)
ΔP	Transmembrane pressure (bar)
R^2	Regression coefficient (dimensionless)
R_{ads}	Resistance due to adsorption on membrane surface and on the pore walls (m^{-1})
$R_{ads,\ ss}$	Resistance due to adsorption at the steady-state (m^{-1})
R_{cl}	Resistance due to the growth of the cake layer (m^{-1})
$R_{cl,\ ss}$	Resistance due to the growth of the cake layer at the steady-state (m^{-1})
R_{cp}	Resistance due to concentration polarization (m^{-1})
$R_{cp,\ ss}$	Resistance due to concentration polarization at the steady-state (m^{-1})
R_m	New membrane resistance (m^{-1})
R_{total}	Total hydraulic resistance (m^{-1})
t	Filtration time (s)

Greek letters

α	Specific cake resistance (m/kg)
μ	Viscosity of the feed solution (kg/m·s)

Abbreviations

BSA	Bovine serum albumin
FD	Fouling degree (%)
LSD	Least Significant Difference
MWCO	Molecular weight cut off
SD	Standard deviation (dimensionless)
WPC	Whey protein concentrate

References

Acevedo-Correa, D., 2010. Gelificatión fría de las proteínas del lactosuero. ReCiTeIA, 10, 1-19.

Argüello, M.A., Álvarez, S., Riera, F.A., Álvarez, R., 2003. Enzymatic cleaning of inorganic ultrafiltration membranes used for whey protein fractionation. J. Membr. Sci., 216, 121–134.

Bacchin, P., Aimar, P., Sanchez, V., 1996. Influence of surface interaction on transfer during colloid ultrafiltration. J. Membr. Sci., 115, 49–63.

Baldasso, C., Barros, T.C., Tessaro, I.C., 2011. Concentration and purification of whey proteins by ultrafiltration. Desalination, 278, 381-386.

Boerlage, S.F.E., Kennedy, M.D., Aniye, M.P., Schippers, J.C., 2003. Applications of the MFI-UF to measure and predict particulate fouling in RO systems. J. Membr. Sci., 220, 97–116.

Bolton, G., LaCasse, D., Kuriyel, R., 2006. Combined models of membrane fouling: development and application to microfiltration and ultrafiltration of biological fluids. J. Membr. Sci., 277, 75-84.

Carbonell-Alcaina, C., Corbatón-Báguena, M.-J., Álvarez-Blanco, S., Bes-Piá, M.A., Mendoza-Roca, J.A., Pastor-Alcañiz, L., 2016. Determination of fouling mechanisms in polymeric ultrafiltration membranes using residual brines from table olive storage wastewaters as feed. J. Food Eng., 187, 14-23.

Carrère, H., Blaszkow, F., Roux de Balmann, H., 2002. Modelling the microfiltration of lactic acid fermentation broths and comparison of operating modes. Desalination, 145, 201-206.

Carrère, H., Blaszkow, F., Roux de Balmann, H., 2001. Modelling the clarification of lactic acid fermentation broths by cross-flow microfiltration. J. Membr. Sci., 186, 219–230.

Carvalho, F., Prazeres, A.R., Rivas, J., 2013. Cheese whey wastewater: Characterization and treatment. Sci. Total Environ., 445-446, 385-396.

Chandrapala, J., Chen, G.Q., Kezia, K., Bowman, E.G., Vasiljevic, T., Kentish, S.E., 2016. Removal of lactate from acid whey using nanofiltration. J. Food Eng., 177, 59-64.

Chen, H., Kim, A.S., 2006. Prediction of permeate flux decline in crossflow membrane filtration of colloidal suspension: a radial basis function neural network approach. Desalination 192, 415-428.

Cheryan, M., Álvarez, J.R., 1995. Chapter 9: Food and beverage industry applications in Noble, R.D., Stern, S.A. (Eds.), Membrane Separations Technology. Principles and Applications. Elsevier Science.

Choi, S.-W., Yoon, J.-Y., Haam, S., Jung, J.-K., Kim, J.-H., Kim, W.-S., 2000. Modeling of the permeate flux during microfiltration of BSA-adsorbed microspheres in a stirred cell. J. Colloid Interface Sci., 228, 270-278.

Corbatón-Báguena, M.-J., Álvarez-Blanco, S., Vincent-Vela, M.C., 2014. Cleaning of ultrafiltration membranes fouled with BSA by means of saline solutions. Sep. Purif. Technol., 125, 1–10.

Corbatón-Báguena, M.-J., Álvarez-Blanco, S., Vincent-Vela, M.-C., Lora-García, J., 2015. Utilization of NaCl solutions to clean ultrafiltration membranes fouled by whey protein concentrates. Sep. Purif. Technol., 150, 95-101.

Daufin, G., Escudier, J.P., Carrère, H., Bérot, S., Fillaudeau, L., Decloux, M., 2001. Recent and emerging applications of membrane processes in the food and dairy industry. Trans. IChemE 79, 89-102.

Evans, P.J., Bird, M.R., Pihlajamäki, A., Nyström, M., 2008. The influence of hydrophobicity, roughness and charge upon ultrafiltration membranes for black tea liquor clarification. J. Membr. Sci., 313, 250–262.

Fernández P., Riera F.A., Álvarez R., Álvarez S., 2010. Nanofiltration regeneration of contaminated single-phase detergents used in the dairy industry. J. Food Eng., 97, 319-328.

García-Ivars, J., Iborra-Clar, M.-I., Alcaina-Miranda, M.-I., Mendoza-Roca, J.-A., Pastor-Alcañiz, L., 2016. Surface photomodification of flat-sheet PES membranes with improved antifouling properties by varying UV irradiation time and additive solution pH. Chem. Eng. J., 283, 231-242.

García-Ivars, J., Alcaina-Miranda, M.-I., Iborra-Clar, M.-I., Mendoza-Roca, J.-A., Pastor-Alcañiz, L., 2014. Enhancement in hydrophilicity of different polymer phaseinversion ultrafiltration membranes by introducing PEG/Al_2O_3 nanoparticles. Sep. Purif. Technol., 128, 45–57.

Garrido, B.C., Souza, G.H.M.F., Lourenço, D.C., Fasciotti, M., 2016. Proteomics in quality control: Whey protein-based supplements. J. Proteomics, 147, 48-55.

Ghosh, R., 2003. Protein bioseparation using ultrafiltration. Theory, applications and new developments, Imperial College Press, London.

Goulas A., Grandison A.S., 2008. Applications of membrane separations in Britz T.J., Robinson R.K., Advanced Dairy Science and Technology, United Kingdom, Blackwell Publishing.

Ho, C.-C., Zydney, A.L., 2000. A combined pore blockage and cake filtration model for protein fouling during microfiltration. J. Colloid Interface Sci., 232, 389-399.

Juang, R.-S., Chen, H.-L., Chen, Y.-S., 2008. Membrane fouling and resistance analysis in dead-end ultrafiltration of Bacillus subtilis fermentation broths. Sep. Purif. Technol., 63, 531-538.

Katsoufidou, K., Yiantsios, S.G., Karabelas, A.J., 2005. A study of ultrafiltration membrane fouling by humic acids and flux recovery by backwashing: Experiments and modelling. J. Membr. Sci., 266, 40-50.

Kazemimoghadam, M., Mohammadi, T., 2006. Chemical cleaning of ultrafiltration membranes in the milk industry. Desalination, 204, 213-218.

Labbez C., Fievet P., Szymczyk A., Vidonne A., Foissy A., Pagetti J., 2002. Analysis of the salt retention of a titania membrane using a "DSPM" model: effect of pH, salt concentration and nature, J. Membr. Sci., 208, 315-329.

Lee, Y., Clark, M.M., 1998. Modeling of flux decline during crossflow ultrafiltration of colloidal suspensions. J. Membr. Sci., 149, 181-202.

Mah, S.-K., Chuah, C.-K., Cathie Lee, W.P., Cahi, S.-P., 2012. Ultrafiltration of palm oil-oleic acid-glycerin solutions: fouling mechanism identification, fouling mechanism analysis and membrane characterizations, Sep. Purif. Technol., 98, 419-431.

Matzinos, P., Álvarez, R., 2002. Effect of ionic strength on rinsing and alkaline cleaning of ultrafiltration inorganic membranes fouled with whey proteins. J. Membr. Sci., 208, 23–30.

Message, J.-L., Blanchard, C., Mint-Dah, F.-V., Lafarge, C., Assifaoui, A., Saurel, R., 2013. The effects of sodium alginate and calcium levels on pea proteins cold-set gelation. Food Hydrocolloids, 31, 446-457.

Metsämuuronen, S., Nyström, M., 2009. Enrichment of α-lactalbumin from diluted whey with polymeric ultrafiltration membranes. J. Membr. Sci., 337, 248-256.

Mo, H., Tay, K.G., Ng, H.Y., 2008. Fouling of reverse osmosis membrane by protein (BSA): effects of pH, calcium, magnesium, ionic strength and temperature. J. Membr. Sci., 315, 28–35.

Mondal, S., De, S., 2010. A fouling model for steady state crossflow membrane filtration considering sequential intermediate pore blocking and cake formation. Sep. Purif. Technol., 75, 222-228.

Rahimpour, A., Madaeni, S.S., 2010. Improvement of performance and surface properties of nano-porous polyethersulfone (PES) membrane using hydrophilic monomers as additives in the casting solution. J. Membr. Sci., 360, 371–379.

Rajabzadeh, A.R., Moresoli, C., Marcos, B., 2010. Fouling behaviour of electroacidified soy protein extracts during cross-flow ultrafiltration using dynamic reversible-irreversible fouling resistances and CFD modelling. J. Membr. Sci., 361, 191-205.

Ramchandran, L., Vasiljevic, T., 2013. Chapter 9: Whey Processing, in Tamine A.Y. (Ed.), Membrane Processing: Dairy and Beverage Applications. Blackwell Publishing, United Kingdom, pp.193-207.

Salahi, A., Abbasi, M., Mohammadi, T., 2010. Permeate flux decline during UF of oily wastewater: experimental and modelling. Desalination, 251, 153–160.

Salinas-Rodríguez, S.G., Amy, G.L., Schippers, J.C., Kennedy, M.D., 2015. The Modified Fouling Index Ultrafiltration constant flux for assessing particulate/colloidal fouling of RO systems. Desalination, 365, 79-91.

Vincent-Vela, M.-C., Álvarez-Blanco, S., Lora-García, J., Bergantiños-Rodríguez, E., 2009. Analysis of membrane pore blocking models adapted to crossflow ultrafiltration in the ultrafiltration of PEG. Chem. Eng. J., 149, 232-241.

Wang, C., Li, Q., Tang, H., Yan, D., Zhou, W., Xing, J., Wan, Y., 2012. Membrane fouling mechanism in ultrafiltration of succinic acid fermentation broth. Biores. Technol., 116, 366–371.

Wen-qiong, W., Lan-wei, Z., Xue, H., Yi, L., 2017. Cheese whey protein recovery by ultrafiltration through transglutaminase (TG) catalysis whey protein cross-linking. Food Chem., 215, 31-40.

Williams, L.J., Abdi, H., 2010. Fisher's Least Significant Difference (LSD) Test in Salkind N. (Ed.): Encyclopedia of Research Desing. Sage, Thousand Oaks, CA.

Yu, W., Xu, L., Graham, N., Qu, J., 2014. Pre-treatment for ultrafiltration: effect of pre-chlorination on membrane fouling. Scientific Reports, 1, 6513.

Zhang, W., Ding, L., Jaffrin, M.Y., Grimi, N., Tang, B., 2016. Stepwise membrane fouling model for shear-enhanced filtration of alfalfa juice: experimental and modelling studies. Royal Soc. Chem. Adv., 6, 110789-110798.

Zin, G., Penha, F.M., Rezzadori, K., Silvia, F.L., Guizoni, K., Petrus, J.C.C., Oliveira, J.V., Di Luccio, M., 2016. Fouling control in ultrafiltration of bovine serum albumin and milk by the use of permanent magnetic field. J. Food Eng., 168, 154-159.

Table 1. Composition of the commercial whey protein concentrate (dry basis)

Component	Concentration (%w)
Dry matter	93.66 ± 0.95
Proteins	40.74 ± 0.79
Lactose	38.27 ± 0.49
Fat	8.14 ± 0.20
Ashes	7.85 ± 0.07
Ca	0.79 ± 0.06
Na	1.21 ± 0.09
K	1.42 ± 0.02
Cl	4.07 ± 0.24
PO_4-P	0.37 ± 0.03

Table 2. Values of the fitting parameters for the resistance-in-series model.

Membrane	Feed solution	$R_{ads,ss}+R_{cp,\ ss}$ ($\cdot 10^{12}$ m^{-1})	b (s^{-1})	$R_{cl,\ ss}$ ($\cdot 10^{12}$ m^{-1})	α ($\cdot 10^{13}$ m/kg)
5 kDa	BSA	2.909	0.232	4.757	5.054
	BSA + $CaCl_2$	14.840	0.238	10.360	17.980
	WPC 22.2 g/L	28.690	0.238	16.200	72.560
	WPC 33.3 g/L	34.190	0.239	15.820	39.050
	WPC 44.4 g/L	33.720	0.239	28.550	29.490
15 kDa	BSA	6.143	0.237	5.896	4.073
	BSA + $CaCl_2$	10.940	0.236	12.070	9.749
	WPC 22.2 g/L	17.510	0.239	16.480	19.110
	WPC 33.3 g/L	19.240	0.240	25.660	25.920
	WPC 44.4 g/L	27.180	0.237	30.900	28.390
30 kDa	BSA	3.104	0.237	2.104	1.448
	BSA + $CaCl_2$	6.741	0.237	2.686	3.394
	WPC 22.2 g/L	12.520	0.237	4.778	8.755
	WPC 33.3 g/L	14.790	0.241	6.248	6.177
	WPC 44.4 g/L	18.970	0.236	7.048	6.624

Table 3. Goodness of fit (in terms of R^2 and SD) for the resistance-in-series model.

Feed solution	5 kDa		15 kDa		30 kDa	
	R^2	SD	R^2	SD	R^2	SD
BSA	0.981	0.014	0.991	0.011	0.996	0.005
BSA + $CaCl_2$	0.986	0.012	0.994	0.011	0.993	0.005
WPC 22.2 g/L	0.982	0.012	0.964	0.025	0.981	0.010
WPC 33.3 g/L	0.980	0.012	0.983	0.022	0.984	0.010
WPC 44.4 g/L	0.956	0.027	0.982	0.021	0.979	0.011

Figure

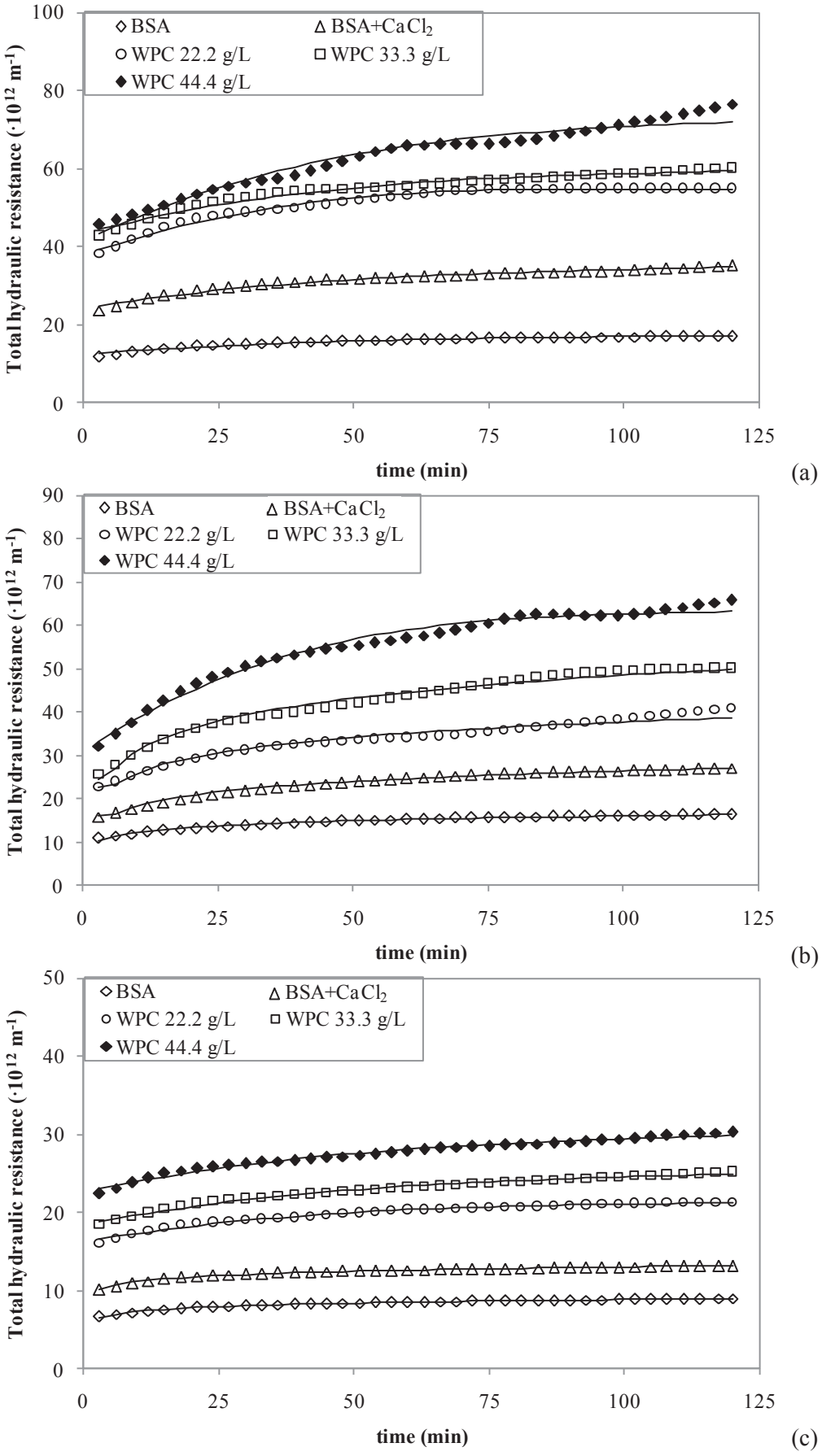

Fig. 1. Time evolution of total hydraulic resistance for all the feed solutions and the (a) 5 kDa, (b) 15 kDa and (c) 30 kDa membranes (solid line: predicted results; symbols: experimental data).

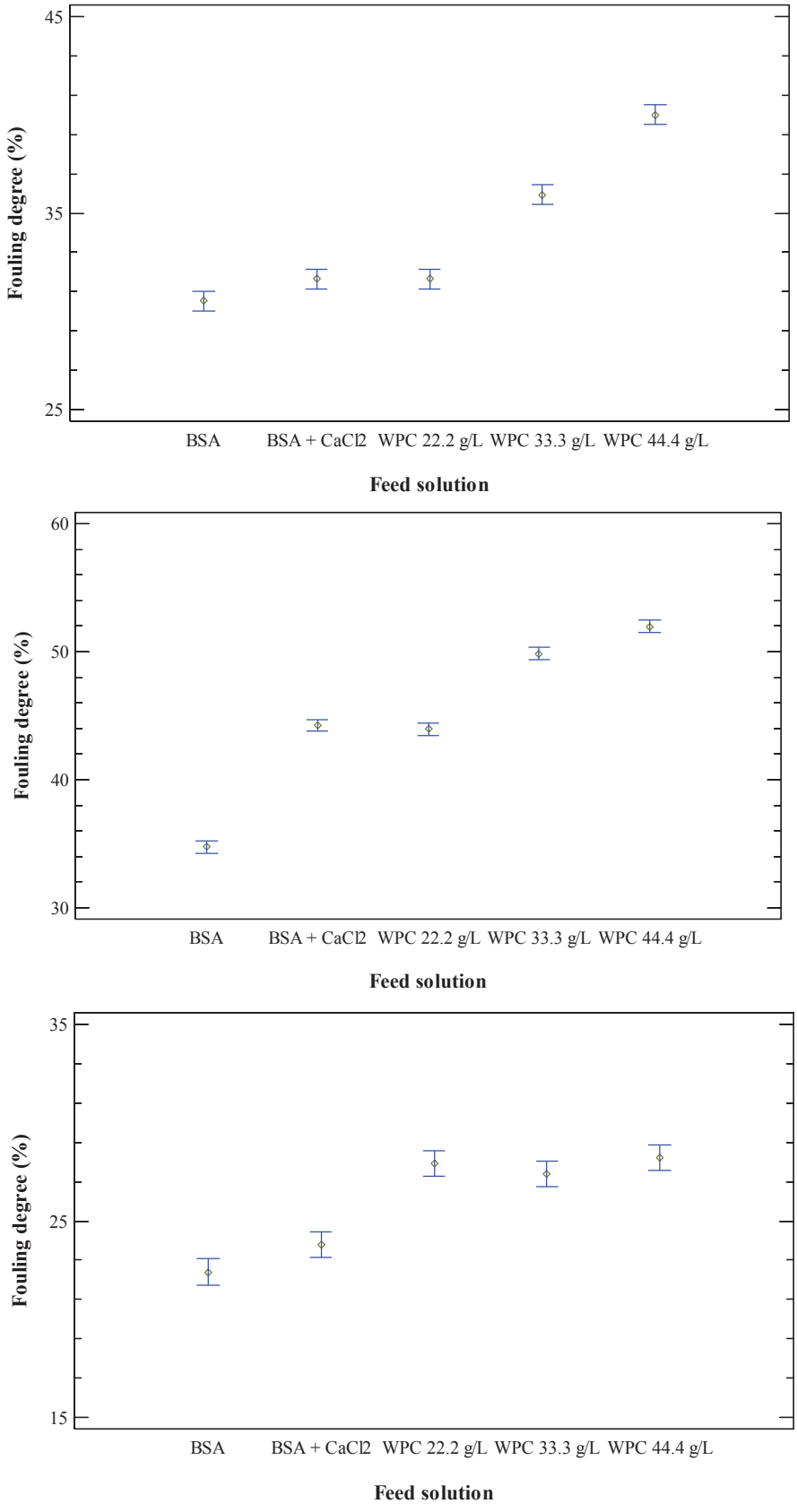

Fig. 2. Least Significant Difference intervals for fouling degree as a function of the different feed solutions tested for the (a) 5 kDa, (b) 15 kDa and (c) 30 kDa.

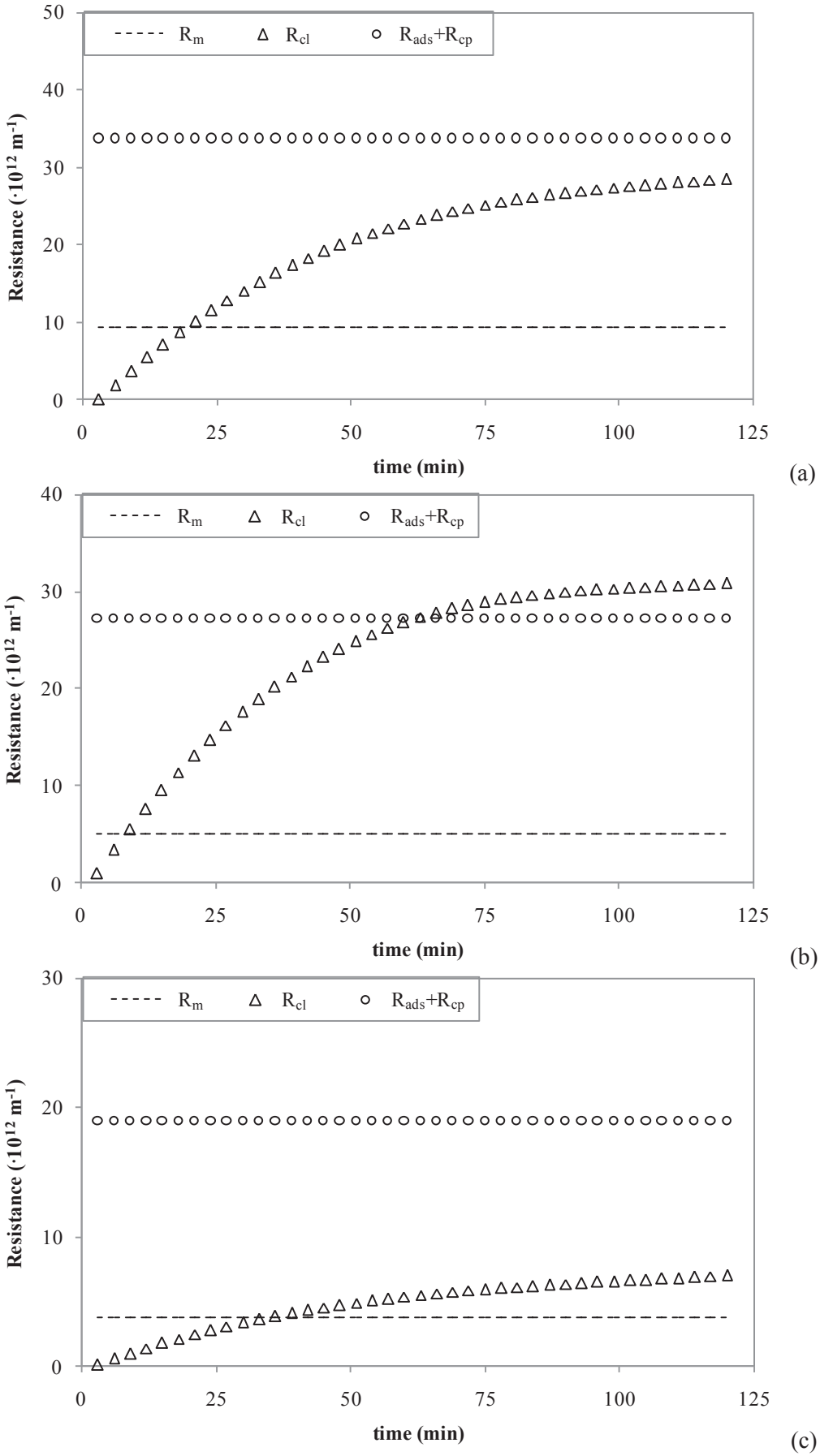

Fig. 3. Time evolution of the fouling resistances for the 44.4 g/L WPC solution and the (a) 5 kDa, (b) 15 kDa and (c) 30 kDa membranes.

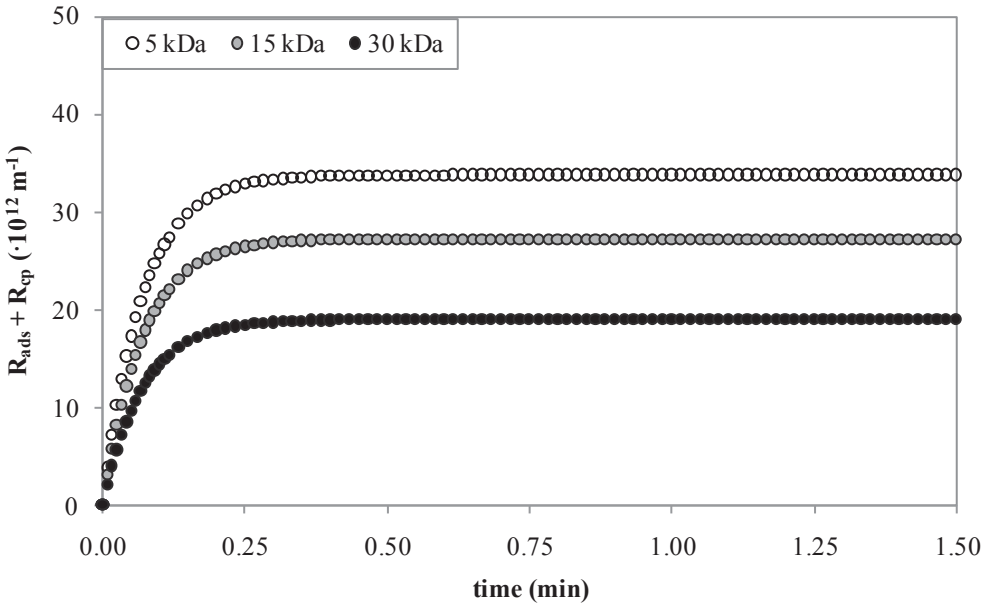

Fig. 4. Initial predicted evolution of the resistance due to adsorption and concentration polarization for the 44.4 g/L WPC solution and the three membranes tested.